Suppression of Superfluid Density and the Pseudogap State in the Cuprates by Impurities

Unurbat Erdenemunkh,[1] Brian Koopman,[1] Ling Fu,[1] Kamalesh Chatterjee,[2] W. D. Wise,[2] G. D. Gu,[3] E. W. Hudson,[4,2] and Michael C. Boyer[1,2,*]

[1]*Department of Physics, Clark University, Worcester, Massachusetts 01610, USA*

[2]*Department of Physics, Massachusetts Institute of Technology, Cambridge, Massachusetts 02139, USA*

[3]*Condensed Matter Physics and Materials Science Department, Brookhaven National Laboratory, Upton, New York 11973, USA*

[4]*Department of Physics, Pennsylvania State University, State College, Pennsylvania 16802, USA*

(Received 16 July 2016; published 16 December 2016)

We use scanning tunneling microscopy (STM) to study magnetic Fe impurities intentionally doped into the high-temperature superconductor $Bi_2Sr_2CaCu_2O_{8+\delta}$. Our spectroscopic measurements reveal that Fe impurities introduce low-lying resonances in the density of states at $\Omega_1 \approx 4$ meV and $\Omega_2 \approx 15$ meV, allowing us to determine that, despite having a large magnetic moment, potential scattering of quasiparticles by Fe impurities dominates magnetic scattering. In addition, using high-resolution spatial characterizations of the local density of states near and away from Fe impurities, we detail the spatial extent of impurity-affected regions as well as provide a local view of impurity-induced effects on the superconducting and pseudogap states. Our studies of Fe impurities, when combined with a reinterpretation of earlier STM work in the context of a two-gap scenario, allow us to present a unified view of the atomic-scale effects of elemental impurities on the pseudogap and superconducting states in hole-doped cuprates; this may help resolve a previously assumed dichotomy between the effects of magnetic and nonmagnetic impurities in these materials.

DOI: 10.1103/PhysRevLett.117.257003

Numerous studies have examined the impact of elemental impurities intentionally doped into high-temperature superconductors so as to understand their pairing mechanism. Early doping studies demonstrated that, in contrast to conventional superconductors, nonmagnetic impurities were more detrimental to superconductivity than magnetic ones [1–3], and this generalization appeared confirmed at the atomic scale by scanning tunneling microscopy (STM) studies [4,5]. Impurities, whether native or intentionally doped into the bulk or at the surface of a superconductor, generate local, low-lying electronic states. These "quasiparticle resonances" have been imaged by STM, which, with its ability to measure spectroscopic maps indicative of the spatially varying local density of states (DOS), allows characterization of their energetic and spatial structure [4–10]. In doped $Bi_2Sr_2CaCu_2O_{8+\delta}$ (BSCCO), STM measurements in the vicinity of "nonmagnetic" Zn impurities find a single impurity resonance near the Fermi energy accompanied by suppressed spectral peaks, interpreted as indicative of the local destruction of superconductivity through strong potential scattering [4]. In contrast, STM measurements near "magnetic" Ni impurities find a split resonance due to an exchange interaction of the quasiparticle spin with the magnetic moment of the Ni impurity atom, as well as complementary particle-hole quasiparticle states, suggesting preservation of superconductivity in the impurity-affected region [5]. These atomic-scale studies suggest marked differences in the local effects of nonmagnetic and magnetic impurities on high-temperature superconductivity. However, since Ni impurities in BSCCO have a relatively small effect on T_C compared to other magnetic impurities such as Fe and Co [11,12], comparative STM studies of other magnetic impurities will allow for a more complete understanding of the relative impact of potential and magnetic scattering by impurities on the superconducting and pseudogap states. Previous STM studies on Fe- and Co-doped BSCCO have been conducted, but lack the spectroscopic details needed for comparison to the previous Zn and Ni impurity studies [13,14].

To address this, we have studied Fe impurities in BSCCO, where, at low concentrations, Fe impurities can reduce T_C at 5 times the rate of Ni impurities [11]. Similar to Zn and Ni, Fe impurities substitute for Cu atoms in the CuO_2 plane. Thermopower measurements indicate that Fe is in the Fe^{2+} ionic state when substituting for Cu^{2+} in the CuO_2 plane, as evidenced by no change in sample hole concentration in near-optimally doped samples for Fe doping of less than ~4% [12]. This indicates that the effects Fe impurities have on bulk T_C are not due to changes in carrier (hole) concentration, but rather are linked to impurity interactions with quasiparticles in the CuO_2 plane. Magnetic susceptibility measurements of Fe impurities (in the $3d^6$, $s = 2$ state) indicate a $\sim 5.2\,\mu_B$ magnetic moment in $Bi_2Sr_2CaCu_2O_{8+\delta}$ [12], considerably larger than the $\sim 1.5\,\mu_B$ estimated magnetic moment of Ni [15].

Our $Bi_{2.1}Sr_{1.9}Ca(Cu_{(1-x)}Fe_x)_2O_{8+\delta}$ samples ($x = 0.005$) have a T_C of 82 K, reduced by the Fe from the 89 K T_C of their slightly oxygen-overdoped parent ($x = 0$) material [16]. We cleave our samples in ultrahigh vacuum at 20 K and immediately insert them into our home-built,

 © 2016 American Physical Society

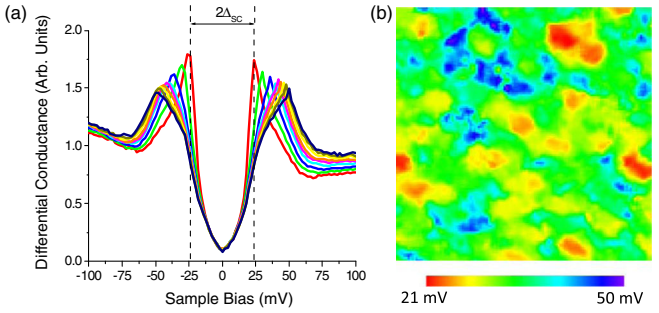

FIG. 1. (a) Spectra group averaged based on Δ_{PG} from the region in (b). In the smallest gapped spectrum, $\Delta_{PG} \approx \Delta_{SC} \approx 24$ mV. Kinks at 24 mV in the larger gap spectra are associated with Δ_{SC}. (b) Gap map over a 200 Å-square region showing standard inhomogeneity of Δ_{PG}. $\Delta_{PG} = 33 \pm 5$ mV. Our values for Δ_{SC} and Δ_{PG} are consistent with reported near-nodal and antinodal gap sizes by ARPES on BSCCO for samples of comparable hole doping [22,23].

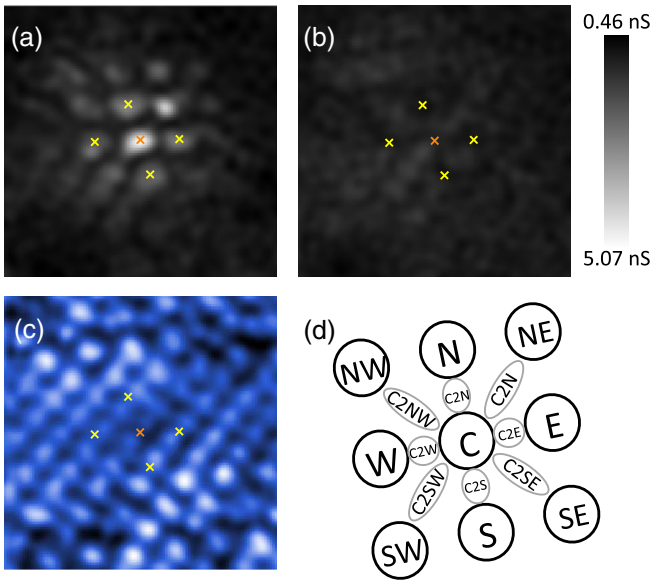

FIG. 2. 33 Å images taken concurrently around a single Fe impurity. (a) +16 mV differential conductance map. An orange x marks the impurity center. Yellow x's indicate the locations of the nearest impurity bright spots to the impurity center [N, E, S, and W locations of (d)]. (b) −16 mV map of the same location. (c) Topography showing the Bi atoms in the Bi-O layer. The impurity center is shifted ∼1.5 Å from the expected Bi atom location. (d) Naming scheme used to identify individual features in the impurity-affected region based on +16 mV map layer. C represents the impurity center. N, E, S, and W are nearest neighbor bright spots. NW, NE, SE, SW are next-nearest-neighbor bright spots.

variable-temperature STM. We initially characterize them by acquiring atomically resolved topographies and high-energy-resolution spectroscopic maps over extended spatial regions. Similar to previous STM work on BSCCO [17–19], we find spectra with a uniform spectral kink at ∼24 mV inside a varying larger gap [Fig. 1(a)]. Following our earlier work [20] in the two-gap scenario [21], we associate the 24 mV kink with the superconducting gap, Δ_{SC}, and the larger gap as the inhomogeneous pseudogap, Δ_{PG} [Fig. 1(b)].

In addition, we find an intragap peak at $\sim +16$ mV, associated with Fe impurities, which we can use to map out their locations [Fig. 2(a)]. Fe impurity resonances display a fourfold symmetric spatial structure similar to previously studied Zn and Ni impurities. More specifically, the "+-shaped" spatial pattern and spatial extent seen at +16 mV for Fe impurities are very similar to the patterns seen near 0 mV for Zn impurities [4] and at positive biases for Ni impurities [5]. Confirming that +16 mV resonances are indeed associated with Fe impurities, we find 81 such resonances at +16 mV over a 500 Å-square region, representing an impurity doping of ∼0.25%, consistent with the nominal Fe doping of 0.5%. Variations from nominal doping arise due to solubility issues as seen in STM measurements of Zn impurities.

Rather than being centered on surface Bi atoms, and hence close to subsurface Cu atoms, as is the case for Zn and Ni impurity resonances [4,5], we find Fe resonances to be centered 1.0–1.5 Å away from the expected site [Fig. 2(c)]. This spatial shift cannot be explained by the presence of a supermodulation, which shifts Cu sites in the CuO_2 plane relative to Bi sites in the Bi-O layer by, at most, 0.4 Å along the a axis [24]. Instead, this surprising shift can be explained by the Fe impurity's differing coordination number on substitution. Cu^{2+} ions in BSCCO have a coordination number of five due to their square-pyramidal oxygen-binding geometry. When substituting for Cu^{2+}, both Zn^{2+} and Ni^{2+} ions can also have a coordination number of five, but such a coordination number is unfavorable for Fe^{2+} [25,26]. Since Fe^{2+} favors a different coordination number (four or six), its introduction can induce local lattice distortions as evidenced by the observed position shift of Fe in our data. A similar explanation was used to explain x-ray measurements detecting increases in a-b-lattice parameters and a decrease in the c-lattice parameter when substituting Co^{3+} for Cu^{2+}; Co^{3+} favors a coordination number of six which induces local lattice distortions [27]. A comparison of c-lattice parameters with doping of Ni, Co, and Fe impurities in BSCCO shows a systematic decrease in the c-lattice parameter with Co and Fe doping, but virtually no change with Ni doping [11], consistent with this explanation and consistent with the differing locations of Ni and Fe impurities as detected by STM. Because of this spatial shift, we utilize a naming scheme which is not tied to Cu sites when describing the spatial evolution of the resonance [Fig. 2(d)]. Despite this spatial shift, the observed DOS modulations are near commensurate with the underlying lattice, as has been previously seen in STM studies of other impurities [4,5,9,10].

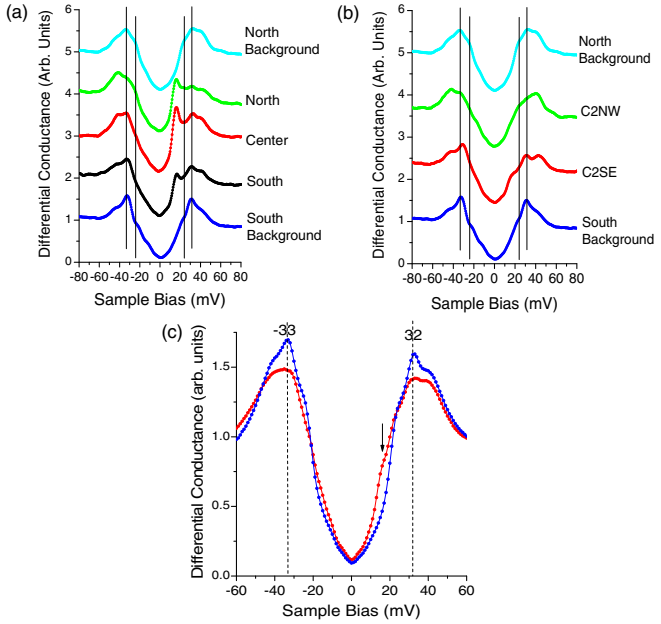

FIG. 3. (a) Background spectra taken directly outside of the impurity-affected region of Fig. 2 (~15 Å from impurity center) show a $\Delta_{SC} \approx 24$ mV kink and peaks indicating $\Delta_{PG} \approx 33$ mV. North, center, and south regions of the impurity-affected region show a single impurity-induced resonance at $\sim +16$ mV. (b) C2NW and C2SE spectra show similar gap-defining peaks but no clear subgap resonances. (c) Overlay of a spatially averaged spectrum taken from within the impurity region (red) with the average local background spectrum (blue). The impurity resonance near +16 mV is clearly seen in the red curve. Both spectra originate from the same 40 Å-square spectral map (33 Å-square region of which appears in Fig. 2). The "local background" spectrum represents an average of spectra from the map which are 15 Å or further away from the impurity center.

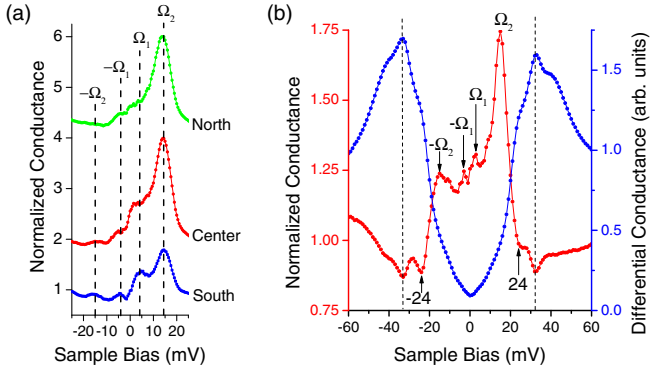

FIG. 4. (a) High-resolution impurity spectra normalized to the local background show two peaks at positive bias: $\Omega_1 \approx 4$ mV and $\Omega_2 \approx 15$ mV. (b) Red: spatially averaged spectrum taken from within the impurity region normalized to the average local background spectrum shows four peaks: ± 3 mV and ± 15 mV. The local background spectrum (blue) provided for reference.

Similar to sample-wide averages, "background" spectra taken directly outside of the Fe impurity location of Fig. 2 show kinks at $\Delta_{SC} \sim 24$ mV and gap edges at $\Delta_{PG} \sim 33$ mV (Fig. 3). Spectra acquired at the north, center, and south regions of the impurity-affected region show an additional impurity-induced resonance at +16 mV [Fig. 3(a)]. Similar to what is observed near Ni impurities, the spectral gap peaks (defining Δ_{PG}) in the Fe impurity-affected region are unchanged from that of the local background [5]. However, these Fe resonances differ from the Ni resonances in two important ways.

First, Ni resonances display spatially complementary particle-hole symmetry [5]; peaks at $+\Omega$ at the center of the resonance move to $-\Omega$ in the "nearest neighbor" locations (C2NW, C2NE, C2SW, and C2SE in our notation). Spatially integrated particle-hole symmetry suggests local preservation of superconductivity [28]. In our measurements, we find no obvious complementary impurity structure at −16 mV [Fig. 2(b)] nor clear evidence for complementary peaks at negative bias in C2NW or C2SE spectra [Fig. 3(b)] or in spectra spatially averaged over the impurity region [Fig. 3(c)]. Compared to Ni impurities, this lack of obvious complementary behavior indicates, at minimum, a partial suppression of superconductivity by Fe impurities. Second, our Fe impurity spectra show no clear evidence for magnetic splitting of the resonance peak. Such splitting, resulting in two same-bias peaks, is both theoretically expected for magnetic impurities [29] and observed in Ni impurities [5].

Looks, however, can be deceiving. In order to enhance subtle spectral features that change spatially, we normalize (divide) our spectra by the local background:

$$G_N(E) = \frac{G_{\text{impurity}}(E)}{G_{\text{background}}(E)}.$$

This normalization reveals an additional impurity resonance at +4 mV [Fig. 4(a)], evidence for the expected interaction of quasiparticle spin with the magnetic moment of the Fe impurity atom. Similar results can be obtained using a subtractive normalization scheme (see Supplemental Material [30]).

To quantify the scattering strength of Fe impurities, we employ the model for quasiparticle potential and magnetic scattering by impurities developed by Salkola *et al.* [29], previously used to quantify STM-studied Zn and Ni resonances [4,5].

$$\frac{\Omega_{1,2}}{\Delta_0} = \frac{-1}{2N_F(U \pm W)\ln|8N_F(U \pm W)|}.$$

Here, $\Omega_{1,2}$ represents the impurity-induced resonance energies, Δ_0 represents the spectral gap size, N_F represents the normal-state density states at the Fermi energy, U represents the Coulomb interaction between a quasiparticle and an impurity atom, and W represents the magnetic interaction between a quasiparticle and the magnetic

TABLE I. Compilation of gap size, Δ_0, impurity peak locations, Ω_1 and Ω_2, and potential ($N_F U$) and magnetic scattering ($N_F W$) by Zn, Fe, and Ni impurities organized by decreasing potential scattering. Zn and Ni data are taken from [4] and [5], respectively. Δ_0 for Fe and Ni represent local gap values; Δ_0 for Zn represents an average gap value over an extended region of the sample.

	Zn	Fe	Ni
Δ_0 (meV)	44	33	28
Ω_1 (meV)	−1.5	4	9.2
Ω_2 (meV)	…	15	18.6
$N_F U$	4.18	−1.14	−0.67
$N_F W$	…	0.48	0.14

moment of the impurity atom. In the two-gap scenario, there is some ambiguity as to whether the superconducting or pseudogap gap value should be used for Δ_0. While the presence of complementary particle- and hole-impurity resonances are set by the presence of the superconducting state [37,38], previous temperature-dependent STM measurements of native impurities in related $Bi_2Sr_2CuO_{6+x}$ clearly indicate that the energy and spatial distribution of the main impurity resonances are set by the pseudogap state, not the superconducting state [10]. For this reason, we set $\Delta_0 = \Delta_{PG}$.

Table I summarizes the potential and magnetic scattering values for Fe impurities in comparison to previously studied Ni and Zn impurities. Previous Zn and Ni calculations [4,5] also set Δ_0 equal to the large spectral gap, which allows for direct comparison of our Fe impurity calculations to those of Zn and Ni. Despite a large magnetic moment, potential scattering dominates magnetic scattering of quasiparticles by Fe impurities, similar to Ni impurities. In comparison to Ni impurities, Fe impurities are both stronger potential (1.7 times larger) and magnetic scatterers (3.4 times larger). The larger magnetic scattering strength of Fe impurities compared to Ni impurities is consistent with its ∼3.5 times larger magnetic moment.

These normalized spectra not only reveal the expected magnetic splitting of the resonance, but also show at least weak spatially integrated particle-hole symmetry. That is, when we normalize a spectrum, spatially averaged across the impurity-affected region to the local background, we find a complementary peak at −15 mV, in addition to the strong resonance at +15 mV, as well as evidence for complementary lower-energy peaks near ±3 mV [Fig. 4(b)]. The presence of these complementary peaks indicates partially preserved particle-hole symmetry in the impurity-affected region, indicating the presence of superconductivity in the immediate vicinity of the impurity.

The spatially averaged normalized impurity spectrum shows two additional important features. First, dips near ±33 mV indicate a suppression of the pseudogap state in the impurity-affected region; the spectral peak heights of the pseudogap state are diminished in the impurity-affected region, but the peak locations are unchanged. This local effect of impurities on the pseudogap state is consistent with Raman measurements on impurity-doped $Bi_2Sr_2CaCu_2O_{8+\delta}$ and $YBa_2Cu_3O_{7-\delta}$; the B_{1g} (antinodal) response peak intensity is diminished, but energy location is unchanged with impurity doping [16,39,40]. Second, while complementary particle-hole resonance peaks indicate the presence of the superconducting state in the impurity-affected region, the clear dip near −24 mV indicates that the coherence peaks associated with superconductivity are partially suppressed. Because the amplitude of coherence peaks is linked to superfluid density [41–44], the observed spectral suppression at Δ_{SC} is consistent with a local suppression of superfluid density near Fe impurities. This would explain T_C suppression with Fe impurity doping.

Our studies allow us to reinterpret previous STM studies of intentionally doped and native impurities. Previous STM measurements on magnetic Ni impurities indicate virtually no local effect on the superconducting state [5], but evidence for partial suppression of the pseudogap state (see Supplemental Material [30]). In contrast, our studies on magnetic Fe impurities show a local partial suppression of both. In fact, the local effects of Fe impurities on these states are more comparable to the local effects of nonmagnetic Zn impurities, when interpreted in the two-gap scenario. Thus, we suggest there is no clear dichotomy between the effects of magnetic and nonmagnetic impurities in BSCCO, but rather that an impurity's ability to suppress superconductivity, in particular superfluid density, is dominated by its potential scattering strength.

The study of Zn-doped $Bi_2Sr_2CaCu_2O_{8+\delta}$ by Pan *et al.* [4] shows background spectra with spectral kinks at ∼25 mV (the superconducting gap), in addition to the spectral peaks at ∼40 mV (the pseudogap). While Zn impurities destroy the latter, the former survive, suggesting strong suppression of the pseudogap by Zn impurities, but locally preserved superconducting order (though reduced superfluid density) with minimal, if any, change in pairing strength. These effects are analogous to what we observe for Fe impurities. This interpretation is consistent with bulk studies indicating both a stronger suppression of the pseudogap state [45–50] and superfluid density [2,51] by Zn impurities than by Ni impurities in the related high-temperature superconductor $YBa_2Cu_3O_{7-\delta}$. Our conclusions are compatible with the "Swiss-cheese" model previously employed to explain muon spin relaxation rate measurements as a function of Zn doping [51]. In this model, it is assumed that the superfluid density is zero around Zn impurities on the length scale of the in-plane coherence length. Our studies suggest that the superfluid density, while diminished, is not zero in the vicinity of Zn impurities, which explains why the Swiss-cheese model appears to slightly underestimate the measured relaxation

rate (proportional to superfluid density) in Zn-doped $YBa_2Cu_3O_{7-\delta}$ [51]. We note that our conclusions are consistent with that of a very recent study of single-crystal films of $La_{2-x}Sr_xCuO_4$ that "T_C seems to be principally controlled by the superfluid density" [52].

This interpretation is also consistent with previous STM studies of native [7,9] and surface impurities [8] in BSCCO which, in addition to the presence of a low-lying impurity resonance, show a narrowing of spectral peaks resulting in a smaller spectral gap. The broad spectral peaks bounding "the gap" in background spectra actually represent the sum of peaks due to the superconducting and pseudogap states. Near impurities, the higher energy pseudogap peaks are significantly suppressed, leaving behind sharper, lower energy, superconducting coherence peaks. Similar to Fe, Ni, and Zn impurities, these native and surface impurities suppress the pseudogap while locally preserving superconductivity, albeit with perhaps some loss of superfluid density.

In each of the hole-doped cuprates $Bi_2Sr_2CaCu_2O_{8+\delta}$, $YBa_2Cu_3O_{7-\delta}$, and $La_{2-x}Sr_xCuO_4$, bulk measurements of single crystals find that, as long as impurity doping levels are low enough that off-Cu-site doping and solubility limits can be ignored, Zn impurities suppress superconductivity (reduce T_C) to a greater extent than Ni impurities [3,53,54]. While Zn impurities have a larger effect on T_C than Fe impurities in BSCCO [11,12,53,55,56], in $La_{2-x}Sr_xCuO_4$, the opposite is true [54]. Resistivity [57] and angle-resolved photoemission spectroscopy [58–60] measurements on Zn impurities in $La_{2-x}Sr_xCuO_4$ on near-optimally and overdoped samples indicate, similar to $Bi_2Sr_2CaCu_2O_{8+\delta}$ and $YBa_2Cu_3O_{7-\delta}$, that Zn impurities are strong potential scatterers near the unitary limit, which can explain T_C suppression with Zn doping consistent with the Swiss-cheese model [51]. Xiao *et al.* initially attributed the stronger suppression of T_C by Fe impurities in $La_{2-x}Sr_xCuO_4$ to magnetic pair breaking due to Fe's larger retained magnetic moment [54]. However, other studies of Ni, Co, and Fe impurities in $La_{2-x}Sr_xCuO_4$ conclude that their retained magnetic moments cannot explain their effect on superconductivity and resulting T_C suppression [61,62]. How these traditionally magnetic impurities disrupt superconductivity and suppress T_C in $La_{2-x}Sr_xCuO_4$ remains an open question, with suggested possibilities including potential scattering by impurities [63,64], carrier localization [61,62], and pair breaking away from nodal regions of the Fermi surface [65]. In addition, the stronger suppression of T_C by Fe than by Zn impurities in $La_{2-x}Sr_xCuO_4$ may reflect the complexities individual to each cuprate family as well as differences between single- and multiple-layer cuprates. Whereas magnetic scattering is the dominant mechanism by which impurities suppress superconductivity in conventional superconductors, our studies suggest it plays only a secondary role to potential scattering in the cuprates. Understanding why the magnetic component of an impurity appears to play such a minor role may ultimately help us to understand what binds together Cooper pairs in these enigmatic superconductors.

We thank Bill Atkinson and Kyle Shen for useful conversations. The authors thank J. C. Davis for access to Zn and Ni doped Bi-2212 data. This work is supported by NSF Grant No. DMR-1341286 and Clark University (university and physics department research student support). The work at BNL was supported by DOE, Office of Science under DE-SC0012704.

*To whom correspondence should be addressed.
mboyer@clarku.edu

[1] K. Ishida, Y. Kitaoka, N. Ogata, T. Kamino, K. Asayama, J. R. Cooper, and N. Athanassopoulou, J. Phys. Soc. Jpn. **62**, 2803 (1993).
[2] D. A. Bonn, S. Kamal, K. Zhang, R. Liang, D. J. Baar, E. Klein, and W. N. Hardy, Phys. Rev. B **50**, 4051 (1994).
[3] K. Tomimoto, I. Terasaki, A. I. Rykov, T. Mimura, and S. Tajima, Phys. Rev. B **60**, 114 (1999).
[4] S. H. Pan, E. W. Hudson, K. M. Lang, H. Eisaki, S. Uchida, and J. C. Davis, Nature (London) **403**, 746 (2000).
[5] E. W. Hudson, K. M. Lang, V. Madhavan, S. H. Pan, H. Eisaki, S. Uchida, and J. C. Davis, Nature (London) **411**, 920 (2001).
[6] A. Yazdani, B. A. Jones, C. P. Lutz, M. F. Crommie, and D. M. Eigler, Science **275**, 1767 (1997).
[7] E. W. Hudson, S. H. Pan, A. K. Gupta, K. W. Ng, and J. C. Davis, Science **285**, 88 (1999).
[8] A. Yazdani, C. M. Howald, C. P. Lutz, A. Kapitulnik, and D. M. Eigler, Phys. Rev. Lett. **83**, 176 (1999).
[9] E. W. Hudson, V. Madhavan, K. McElroy, J. E. Hoffman, K. M. Lang, H. Eisaki, S. Uchida, and J. C. Davis, Physica (Amsterdam) **329B–333B**, 1365 (2003).
[10] K. Chatterjee, M. C. Boyer, W. D. Wise, T. Kondo, T. Takeuchi, H. Ikuta, and E. W. Hudson, Nat. Phys. **4**, 108 (2008).
[11] T. D. Hien, N. K. Man, and K. B. Garg, J. Magn. Magn. Mater. **262**, 508 (2003).
[12] T. M. Benseman, J. R. Cooper, C. L. Zentile, L. Lemberger, and G. Balakrishnan, Phys. Rev. B **84**, 144503 (2011).
[13] S. Baar, N. Momono, J. Suzuki, J. Soda, K. Kobayashi, H. Takano, Y. Amakai, T. Kurosawa, M. Oda, and M. Ido, Phys. Procedia **75**, 18 (2015).
[14] H. Ichikawa, Y. Kobayashi, T. Sakuraba, H. Shibata, and A. Matsuda, Physica (Amsterdam) **469C**, 1013 (2009).
[15] P. Mendels, H. Alloul, G. Collin, N. Blanchard, J. F. Marucco, and J. Bobroff, Physica (Amsterdam) **235C–240C**, 1595 (1994).
[16] O. V. Misochko and G. Gu, Phys. Rev. B **59**, 11183 (1999).
[17] C. Howald, P. Fournier, and A. Kapitulnik, Phys. Rev. B **64**, 100504 (2001).
[18] K. M. Lang, V. Madhavan, J. E. Hoffman, E. W. Hudson, H. Eisaki, S. Uchida, and J. C. Davis, Nature (London) **415**, 412 (2002).

[19] J. W. Alldredge, J. Lee, K. McElroy, M. Wang, K. Fujita, Y. Kohsaka, C. Taylor, H. Eisaki, S. Uchida, P. J. Hirschfeld, and J. C. Davis, Nat. Phys. **4**, 319 (2008).
[20] M. C. Boyer, W. D. Wise, K. Chatterjee, M. Yi, T. Kondo, T. Takeuchi, H. Ikuta, and E. W. Hudson, Nat. Phys. **3**, 802 (2007).
[21] S. Hüfner, M. A. Hossain, A. Damascelli, and G. A. Sawatzky, Rep. Prog. Phys. **71**, 062501 (2008).
[22] W. S. Lee, I. M. Vishik, K. Tanaka, D. H. Lu, T. Sasagawa, N. Nagaosa, T. P. Devereaux, Z. Hussain, and Z. X. Shen, Nature (London) **450**, 81 (2007).
[23] I. M. Vishik, M. Hashimoto, R. H. He, W. S. Lee, F. Schmitt, D. Lu, R. G. Moore, C. Zhang, W. Meevasana, T. Sasagawa, S. Uchida, K. Fujita, S. Ishida, M. Ishikado, Y. Yoshida, H. Eisaki, Z. Hussain, T. P. Devereaux, and Z. X. Shen, Proc. Natl. Acad. Sci. U.S.A. **109**, 18332 (2012).
[24] Y. Gao, P. Lee, P. Coppens, M. A. Subramania, and A. W. Sleight, Science **241**, 954 (1988).
[25] R. D. Shannon and C. T. Prewitt, Acta Crystallogr. Sect. B **25**, 925 (1969).
[26] R. Shannon, Acta Crystallog. Sect. A **32**, 751 (1976).
[27] A. Özaslan, B. Özçelik, B. Özkurt, A. Sotelo, and M. A. Madre, J. Supercond. Novel Magn. **27**, 53 (2014).
[28] M. E. Flatté, Phys. Rev. B **61**, R14920 (2000).
[29] M. I. Salkola, A. V. Balatsky, and J. R. Schrieffer, Phys. Rev. B **55**, 12648 (1997).
[30] See Supplemental Material at http://link.aps.org/supplemental/10.1103/PhysRevLett.117.257003, which include Refs. [31–36], for additional analysis of the spatial shifts of Fe impurities, the application of the division normalization technique to Zn and Ni data, and a comparison of division and subtraction normalization techniques.
[31] M. Fujita, H. Hiraka, M. Matsuda, M. Matsuura, J. M. Tranquada, S. Wakimoto, G. Xu, and K. Yamada, J. Phys. Soc. Jpn. **81**, 011007 (2012).
[32] M. Kofu, H. Kimura, and K. Hirota, Phys. Rev. B **72**, 064502 (2005).
[33] R. H. He *et al.*, Phys. Rev. Lett. **107**, 127002 (2011).
[34] H. Hiraka *et al.*, Phys. Rev. B **81**, 144501 (2010).
[35] M. Matsuura, M. Fujita, H. Hiraka, M. Kofu, H. Kimura, S. Wakimoto, T. G. Perring, C. D. Frost, and K. Yamada, Phys. Rev. B **86**, 134529 (2012).
[36] A. Suchaneck *et al.*, Phys. Rev. Lett. **105**, 037207 (2010).
[37] A. V. Balatsky, I. Vekhter, and J. X. Zhu, Rev. Mod. Phys. **78**, 373 (2006).
[38] H. V. Kruis, I. Martin, and A. V. Balatsky, Phys. Rev. B **64**, 054501 (2001).
[39] M. Le Tacon, A. Sacuto, Y. Gallais, D. Colson, and A. Forget, Phys. Rev. B **76**, 144505 (2007).
[40] N. Murai, T. Masui, M. Ishikado, S. Ishida, H. Eisaki, S. Uchida, and S. Tajima, Phys. Rev. B **85**, 020507 (2012).
[41] T. Kondo, R. Khasanov, T. Takeuchi, J. Schmalian, and A. Kaminski, Nature (London) **457**, 296 (2009).
[42] D. L. Feng, D. H. Lu, K. M. Shen, C. Kim, H. Eisaki, A. Damascelli, R. Yoshizaki, J. i. Shimoyama, K. Kishio, G. D. Gu, S. Oh, A. Andrus, J. O'Donnell, J. N. Eckstein, and Z. X. Shen, Science **289**, 277 (2000).
[43] B. Sacepe, T. Dubouchet, C. Chapelier, M. Sanquer, M. Ovadia, D. Shahar, M. Feigel'man, and L. Ioffe, Nat. Phys. **7**, 239 (2011).
[44] Y. He, Y. Yin, M. Zech, A. Soumyanarayanan, M. M. Yee, T. Williams, M. C. Boyer, K. Chatterjee, W. D. Wise, I. Zeljkovic, T. Kondo, T. Takeuchi, H. Ikuta, P. Mistark, R. S. Markiewicz, A. Bansil, S. Sachdev, E. W. Hudson, and J. E. Hoffman, Science **344**, 608 (2014).
[45] G.-Q. Zheng, T. Odaguchi, T. Mito, Y. Kitaoka, K. Asayama, and Y. Kodama, J. Phys. Soc. Jpn. **62**, 2591 (1993).
[46] G.-Q. Zheng, T. Odaguchi, Y. Kitaoka, K. Asayama, Y. Kodama, K. Mizuhashi, and S. Uchida, Physica (Amsterdam) **263C**, 367 (1996).
[47] T. Miyatake, K. Yamaguchi, T. Takata, N. Koshizuka, and S. Tanaka, Phys. Rev. B **44**, 10139 (1991).
[48] A. V. Puchkov, D. N. Basov, and T. Timusk, J. Phys. Condens. Matter **8**, 10049 (1996).
[49] G. V. M. Williams, J. L. Tallon, and R. Meinhold, Phys. Rev. B **52**, R7034 (1995).
[50] G. V. M. Williams, J. L. Tallon, R. Dupree, and R. Michalak, Phys. Rev. B **54**, 9532 (1996).
[51] B. Nachumi, A. Keren, K. Kojima, M. Larkin, G. M. Luke, J. Merrin, O. Tchernyshöv, Y. J. Uemura, N. Ichikawa, M. Goto, and S. Uchida, Phys. Rev. Lett. **77**, 5421 (1996).
[52] I. Božović, X. He, J. Wu, and A. T. Bollinger, Nature (London) **536**, 309 (2016).
[53] A. Maeda, T. Yabe, S. Takebayashi, M. Hase, and K. Uchinokura, Phys. Rev. B **41**, 4112 (1990).
[54] G. Xiao, M. Z. Cieplak, J. Q. Xiao, and C. L. Chien, Phys. Rev. B **42**, 8752 (1990).
[55] N. Nomono, T. Kurosawa, M. Naito, M. Oda, M. Ido, Y. Aamakai, H. Takano, S. Murayama, and A. Sakai, J. Phys. Conf. Ser. **150**, 052167 (2009).
[56] M. Akoshima, T. Noji, Y. Ono, and Y. Koike, Phys. Rev. B **57**, 7491 (1998).
[57] Y. Fukuzumi, K. Mizuhashi, K. Takenaka, and S. Uchida, Phys. Rev. Lett. **76**, 684 (1996).
[58] T. Yoshida, X. J. Zhou, Z. Hussain, Z. X. Shen, A. Fujimori, S. Komiya, Y. Ando, H. Eisaki, and S. Uchida, Physica (Amsterdam) **460C–462C**, 872 (2007).
[59] K. Terashima, T. Sato, K. Nakayama, T. Arakane, T. Takahashi, M. Kofu, and K. Hirota, Phys. Rev. B **77**, 092501 (2008).
[60] T. Yoshida, S. Komiya, X. J. Zhou, K. Tanaka, A. Fujimori, Z. Hussain, Z. X. Shen, Y. Ando, H. Eisaki, and S. Uchida, Phys. Rev. B **80**, 245113 (2009).
[61] C. Zhang and Y. Zhang, J. Phys. Condens. Matter **14**, 9659 (2002).
[62] J. Lu, L. Pi, S. Tan, and Y. Zhang, Physica (Amsterdam) **470C**, 1920 (2010).
[63] Y. Tanabe, T. Adachi, K. Suzuki, T. Kawamata, Risdiana T. Suzuki, I. Watanabe, and Y. Koike, Phys. Rev. B **83**, 144521 (2011).
[64] T. Nakano, N. Momono, T. Nagata, M. Oda, and M. Ido, Phys. Rev. B **58**, 5831 (1998).
[65] T. Kurosawa, N. Momono, M. Oda, and M. Ido, Phys. Rev. B **85**, 134522 (2012).